Biosensors and Bioelectronics 59 (2014) 145–150

Contents lists available at ScienceDirect

Biosensors and Bioelectronics

journal homepage: www.elsevier.com/locate/bios

An efficient biosensor made of an electromagnetic trap and a magneto-resistive sensor

Fuquan Li *, Jürgen Kosel

Computer, Electrical and Mathematical Sciences and Engineering Division (CEMSE), King Abdullah University of Science and Technology (KAUST), Thuwal, Saudi Arabia

ARTICLE INFO

Article history:
Received 29 November 2013
Received in revised form
6 March 2014
Accepted 7 March 2014
Available online 28 March 2014

Keywords:
Magnetic biosensor
Electromagnetic trap
Magneto-resistive sensor
Magnetic beads
E. coli detection

ABSTRACT

Magneto-resistive biosensors have been found to be useful because of their high sensitivity, low cost, small size, and direct electrical output. They use super-paramagnetic beads to label a biological target and detect it via sensing the stray field. In this paper, we report a new setup for magnetic biosensors, replacing the conventional "sandwich" concept with an electromagnetic trap. We demonstrate the capability of the biosensor in the detection of *E. coli*. The trap is formed by a current-carrying microwire that attracts the magnetic beads into a sensing space on top of a tunnel magneto-resistive sensor. The sensor signal depends on the number of beads in the sensing space, which depends on the size of the beads. This enables the detection of biological targets, because such targets increase the volume of the beads. Experiments were carried out with a 6 μm wide microwire, which attracted the magnetic beads from a distance of 60 μm, when a current of 30 mA was applied. A sensing space of 30 μm in length and 6 μm in width was defined by the magnetic sensor. The results showed that individual *E. coli* bacterium inside the sensing space could be detected using super-paramagnetic beads that are 2.8 μm in diameter. The electromagnetic trap setup greatly simplifies the device and reduces the detection process to two steps: (i) mixing the bacteria with magnetic beads and (ii) applying the sample solution to the sensor for measurement, which can be accomplished within about 30 min with a sample volume in the μl range. This setup also ensures that the biosensor can be cleaned easily and re-used immediately. The presented setup is readily integrated on chips via standard microfabrication techniques.

1. Introduction

Pathogen detection is of great importance in the food industry, water and environmental monitoring, and clinical diagnosis (Lazcka et al., 2007). Rapid, selective and sensitive pathogen detection is essential to ensure the safety of food and water or to quickly diagnose bacterial diseases. Conventional, standard pathogen detection methods include polymerase chain reaction (PCR), culture and colony counting methods, and immunological methods. PCR and the culture and colony counting methods are the most frequently used, due to their sensitivity, selectivity and reliability. Immunological methods employ antibody–antigen reactions for pathogen detection. The most popular immunological method is the enzyme-linked immunosorbent assay (ELISA), which takes advantages of the specificity of the antibody and the sensitivity of the enzyme assay (Lazcka et al., 2007). However, these methods are very time-consuming (several hours or up to several days (Lazcka et al., 2007)) and require highly skilled technicians and well-equipped biological laboratories. In this context, biosensors are considered as promising alternatives for pathogen detection in the future, but further work is required to make them more reliable, selective and sensitive.

Biosensors usually employ optical (Narsaiah et al., 2011), electrochemical (Lang et al., 2013), piezoelectric (Guo et al., 2012) or magnetic (Baselt et al., 1998; Gaster et al., 2011a,b, 2011c) transducers to detect pathogens. Optical biosensors have exhibited high sensitivity (Velusamy et al., 2010). The most sensitive optical biosensor can achieve a detection limit of 1 cfu/mL *E. coli* O157:H7 within about half an hour (Mechery et al., 2006). However, such a sensor requires a suitable spectrometer or camera, which is expensive and rather large for integrated, compact devices. Electrochemical biosensors have the advantages of low cost and small size, but their sensitivity and selectivity are usually lower compared to optical biosensors. With the help of magnetic bead conjugation and concentration, it is possible to detect 10 cfu/mL *E. coli* O157:H7 using a nanoporous membrane-based electrochemical biosensor (Chan et al., 2013). Piezoelectric biosensors measure changes of the resonant frequency of a quartz

* Corresponding author.
E-mail address: fuquan.li@kaust.edu.sa (F. Li).

http://dx.doi.org/10.1016/j.bios.2014.03.035
0956-5663/

crystal when the biological targets are captured on a bio-functionalized crystal surface. The measurement can take up to a day and requires an enrichment step to reach the detection limit of 10 cfu/mL for *E. coli* O157:H7 (Guo et al., 2012). Without the enrichment step, the detection limit of the piezoelectric biosensor is typically about 10^3 cfu/mL (Buchatip et al., 2010; Su and Li, 2004).

Magnetic biosensors are suitable for very sensitive pathogen detection, because they can provide a resolution that is sufficient to recognize individual magnetic beads (Shen et al., 2005). In addition, magnetic beads can be concentrated or separated by magnetic fields (Gooneratne et al., 2012, 2013), enabling simple expansion of device functionalities.

Commonly, magnetic biosensors utilize the "sandwich" detection scheme, i.e., the target is sandwiched between a bio-functionalized sensor surface and bio-functionalized magnetic beads. This method requires bio-functionalizing the sensor surface and washing the sensor several times to remove extra beads and extra reagents during the measurement. While the method is very sensitive, it is also complex and tedious and an improvement is desirable to simplify the detection procedure, making it faster, more user-friendly and suitable for point-of-care devices. A step in this direction has recently been proposed with the "autoassembly immunoassay" (Gaster et al. 2011a,b, 2011c). In this case, biological targets and magnetic nanoparticles are mixed in the same solution and applied to the biosensor, where they bind to the bio-functionalized sensor's surface. This scheme has been employed for the detection of protein and DNA.

In this paper, we introduce a very simple electromagnetic trap to attract magnetic beads or magnetic bead-biological target compounds on top of a magnetic sensor. In the case of compounds, fewer magnetic beads will be trapped on top of the sensor, since some space will be occupied by the biological targets, leading to smaller output voltages. A higher concentration of biological targets causes more biological targets to bind to magnetic beads, reducing the number of beads inside the electromagnetic trap and resulting in a smaller sensor output. Hence, the concentration of biological targets can be related to the sensor's output. The main advantages of this method are that there is no need to bio-functionalize the sensor's surface and that the sensor works with a simplified detection process that requires only two steps. Since our biosensor is not functionalized, it can easily be cleaned and re-used. Moreover, continuous monitoring operations are also feasible. In this paper, our trap concept is demonstrated for the detection of *E. coli* bacteria.

2. Materials and methods

2.1. Electromagnetic trap

The device consists of a tunnel magneto-resistive (TMR) sensor (details in supplementary material), connected via four electric contacts, with a centrally tapered gold microwire on top of it (Fig. 1a). The microwire is fabricated using standard microfabrication techniques in which sputter deposition is used to deposit 20 nm Ti and 280 nm Au sequentially on top of the magnetic sensor, which is covered by a 200 nm thick silicon nitride layer. A photoresist layer is spin-coated on top and photolithographically patterned. The Ti/Au layer is then dry etched to fabricate the microwire. A 400 nm-thick layer of polymer (Micro-Chemicals, AZ 1505) is spin-coated on top of the gold layer to minimize the adherence of magnetic beads to the chip's surface. The electromagnetic trap is realized by applying a 30 mA electric current in the microwire that generates a non-uniform magnetic field, attracting magnetic beads and immobilizing them.

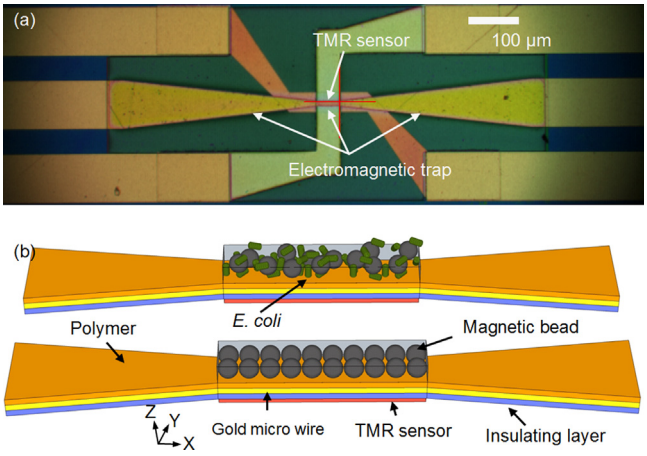

Fig. 1. A magnetic biosensor comprised of an electromagnetic trap and a tunnel magneto-resistive (TMR) sensor: (a) an optical image of the magnetic biosensor. The pads (not shown) for the electrical connections are about 3.7 mm away from the TMR sensor. (b) Schematic of the detection method. The current in the microwire creates a non-uniform magnetic field, forming an electromagnetic trap on top of the TMR sensor. The transparent box filled with magnetic beads represents the sensing space of the TMR sensor, which is the area from which magnetic beads influence the signal of the TMR sensor.

The number of beads trapped on top of the sensor depends on the size of the beads, which changes when biological targets are attached (Fig. 1b).

The size of the electromagnetic trap is defined by the magnetic force, F_{mag}, acting on a superparamagnetic bead, which is dominant over the Brownian force. F_{mag} can be calculated as (Boyer, 1988)

$$F_{mag} = \nabla(mB) = V\chi\nabla(HB), \tag{1}$$

where m is the magnetic moment of the bead, V is its volume, and χ is its susceptibility. Our numerical analysis shows that magnetic beads can be attracted from a distance of 70 μm, which corresponds very well to the 60 μm found experimentally (details provided in the supplementary material). The size of the electromagnetic trap can be adjusted by the design of the microwire, the amount of current and the type of magnetic bead.

2.2. Signal measurement

To increase the signal-to-noise ratio (SNR), a frequency modulation method is employed (de Boer et al., 2007). The beads are magnetized by applying a magnetization current

$$I_M(t) = \sqrt{2} I_M \cos(2\pi f_M t), \tag{2}$$

with an root-mean-square (rms) value of I_M=30 mA and a frequency of f_M=330 Hz to the microwire using a function generator (Agilent, 33250A). At the same time, a sensing current

$$I_S(t) = \sqrt{2} I_S \cos(2\pi f_S t), \tag{3}$$

with an rms value of I_S=400 μA and a frequency of f_S=65 Hz is applied to the TMR sensor using the same function generator (Agilent, 33250A).

The sensor voltage contains the signal of the magnetic beads at f_S+f_M and f_S-f_M (details in the supplementary material). With the help of a lock-in amplifier (Stanford Research, *SR850*), the output voltage, V_{out}, is measured at a frequency of f_S+f_M=395 Hz with a bandwidth of 0.26 Hz:

$$V_{out} = V_M + V_{Stray} = \frac{1}{\sqrt{2}} I_S R_0 \delta(\overline{B_M} + \overline{B_{Stray}}). \tag{4}$$

It includes two components: the voltage, V_M, due to the magnetic field generated by the current of the microwire, and the voltage, V_{Stray}, due to the stray field of the magnetic beads inside the sensing space of the TMR sensor. B_M is the rms value of the magnetic flux density generated by the current in the microwire, and $\overline{B_M}$ is the average value of B_M over the free layer of the magnetic sensor. B_{Stray} is the rms value of the magnetic flux density of the magnetic beads inside the sensing space of the TMR sensor, and $\overline{B_{Stray}}$ is the average value of B_{Stray} over the free layer of the magnetic sensor. R_0 is the base resistance (resistance without a magnetic field) of the magnetic sensor and its sensitivity, δ.

The magnetizing current, I_M, in the microwire generates a non-uniform magnetic field, B_M, forming the electromagnetic trap. This magnetic field also changes the output voltage of the underlying magnetic sensor. The sensitivity, δ, of the TMR sensor can be obtained from Eq. (4) by applying a known value of a magnetic field to the sensor using the microwire. To this end, the value of I_M is swept from 0 mA to 40 mA, in order to study the sensitivity, δ, at a magnetic field of variable strength. A three-dimensional (3D) model is used to calculate $\overline{B_M}$ for a certain value of I_M, and the microwire has a total length of 90 μm. The length and width of the center part are 30 μm and 6 μm, respectively. At the edge, the width is 13.2 μm and the width gradually decreases to 6 μm toward the center. The thickness of the microwire is 0.3 μm. The entire model is contained inside a box that is 120 μm × 30 μm × 30 μm for which the tangential components of the magnetic vector potential at the boundary are set to zero.

To determine the distance from which the magnetic beads can be detected by the magnetic sensor, we investigated the output voltage caused by an individual magnetic bead. Taking into account only the stray field, the voltage can be found from Eq. (4) as

$$V_{Stray} = \frac{1}{\sqrt{2}} I_S R_0 \delta \overline{B_{Stray}}. \quad (5)$$

Another 3D model is used to calculate $\overline{B_{Stray}}$. The model is the same as that for calculating the magnetic field, $\overline{B_M}$, except that: (i) the current is 30 mA, which is the value used in the *E. coli* detection experiments; (ii) a superparamagnetic bead with a diameter of 2.8 μm and a magnetic susceptibility of 0.79 is added to the model.

2.3. E. coli detection

The magnetic beads used in the experiments are Dynabeads® M-270 Streptavidin (Invitrogen). They are superparamagnetic with a diameter of 2.8 μm and a magnetic susceptibility of 0.79 (Li and Kosel, 2013). The surface of the beads is covalently coated with a monolayer of streptavidin.

The magnetic beads are bio-functionalized by incubating them with biotinylated anti-*E. coli* antibodies. The biotinylated anti-*E. coli* antibody, referred to as "Anti-*E. coli* antibody (Biotin) (ab20640)", has specificity for many "O" and "K" antigenic serotypes of *E. coli* and is tested specifically with the strains O18, O20, O44, O55, O111, O112, O125, O157, K12.

Before bio-functionalization, the magnetic beads are washed three times to remove preservatives. We place 100 μL of magnetic bead solution with a concentration of 6.5×10^8 beads/mL into a tube, and then the tube is placed on a magnet for 2 min. The supernatant is then removed by aspiration with a pipette while the tube is kept on the magnet. After removing the tube from the magnet, 100 μL of washing buffer (1 × PBS & 0.05% Tween20) is added and the magnetic beads are re-suspended. These steps are repeated twice more. To the washed magnetic beads, 0.5 μL anti-*E. coli* antibody solution is added for 30 min at room temperature under gentle rotation. The magnetic beads are then washed three times to remove excess antibodies, and the same procedure is applied as before when removing preservatives. Finally, the bio-functionalized magnetic beads are re-suspended in 100 μL of buffer solution (1 × PBS and 0.05% Tween20).

The bacteria are obtained by scratching the inner wall of a toilet bowl with a cotton swab, from which they are transferred to a tube containing 100 μL of solution (1 × PBS and 0.05% Tween20). After adding 5 μL of bio-functionalized magnetic bead solution, the tube is placed on a magnet for 2 min and the supernatant is removed. Next, 100 μL of washing buffer (1 × PBS and 0.05% Tween20) is added and the magnetic beads are re-suspended. This procedure is repeated three times. The magnetic beads are then transferred to a tube containing 2 mL Terrific Broth (modified) and incubated at 37 °C for 18 h. After removing the magnetic beads, the bacteria are kept at −20 °C for long-term storage.

Samples for the experiments are prepared by adding 5 μL of bacteria sample to 2 mL Terrific Broth (modified) and incubating at 37 °C for 18 h. The concentration of *E. coli* is measured with a spectrophotometer (Thermo Scientific, NanoDrop 2000c), and different concentrations are prepared by diluting with deionised water. Then, 5 μL of bio-functionalized bead solution with a concentration of 6.5×10^8 beads/mL is mixed with 95 μL of *E. coli* solution and incubated at room temperature for 30 min. This produces a sample solution containing bare beads and bead-*E. coli* compounds (Fig. 2), which varies in different experiments depending on the concentration of the *E. coli*.

At the beginning of each measurement, the magnetizing and sensing current are applied and the sensor output voltage is recorded. Then, 1 μL of deionized water is applied to the sensor

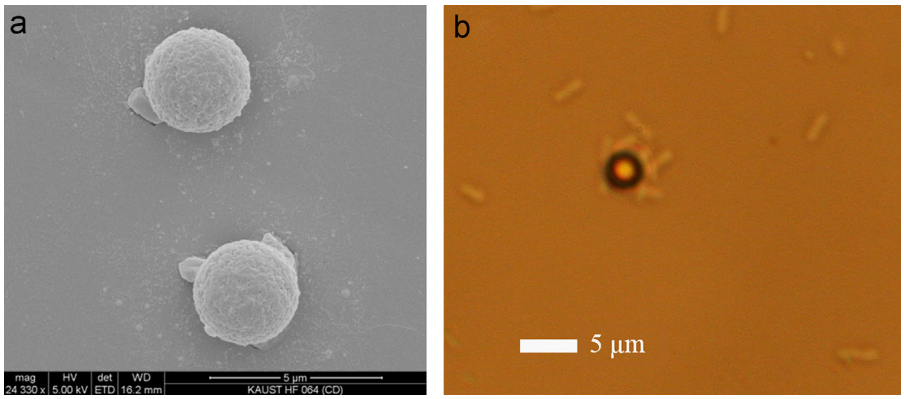

Fig. 2. Streptavidin-coated superparamagnetic beads bound to *E. coli* bacteria via biotinylated anti-*E. coli* antibody (ab20640): (a) SEM image and (b) optical image. Note that the *E. coli* in the SEM image looks smaller than the actual size because it shrinks under the vacuum environment of the SEM chamber.

surface to stabilize the temperature of the sensor, which is slightly raised by the Ohmic losses of the currents. After 60 s, a 1 μL droplet of sample solution is added, and the output voltage is recorded for another 4 min. The average voltage measured over the first 60 s is calculated. This "bias" value is then subtracted from all other values to obtain the actual signal values. The experiment is repeated three times for each sample solution. Between each measurement, the device is washed with deionized water.

3. Results and discussion

3.1. Sensor sensitivity

Fig. 3 shows the sensor's output voltage as a function of the current applied to the microwire, which produces a magnetic field at the sensor. The sensor shows a linear response with a slope of 0.762 μV/mA. The value of B_M produced by a magnetizing current of 1 mA (rms) is obtained from the finite element (FEM) simulation, and its average value over the free layer of the magnetic sensor is $\overline{B_M}$ = 0.9306 G. Hence, using Eq. (4) and the base resistance of the magnetic sensor of 3.6 Ω leads to a sensitivity of δ = 0.804%/mT.

3.2. Simulation of E. coli detection

Fig. 4 shows the voltage, V_{Stray}, caused by an individual magnetic bead and its dependence on the bead's location. For one bead on the chip's surface at the center of the microwire (Y = 0 μm, Z = 1.4 μm), V_{Stray} will be 87.52 nV. This represents the highest value that can be expected from an individual bead. For a bead located somewhere along the edge of the microwire ($Y = \pm 1.5$ μm, Z = 1.4 μm), V_{Stray} is about 60 nV. For a bead located next to the sensor ($Y = \pm 4.5$ μm, Z = 1.4 μm), it drops to about 9 nV. In case the surface is already covered with a layer of beads, additional beads can be trapped in another layer on top of it. A magnetic bead above the center of the sensor in the second layer (Y = 0 μm, Z = 4.2 μm) has a V_{Stray} of 12.42 nV and the value drops drastically for beads further away from the center.

Summarizing the above, when the TMR sensor is fully covered with magnetic beads, two rows of magnetic beads in the first layer contribute ($Y = \pm 1.5$ μm, Z = 1.4 μm) the most to the total signal. Because, essentially, only beads within this space of 30 μm × 6 μm × 2.8 μm will be detected, it is denoted as the sensing space. In total, the sensing space can hold 20 beads, and the total signal generated by those beads should be around 1.2 μV.

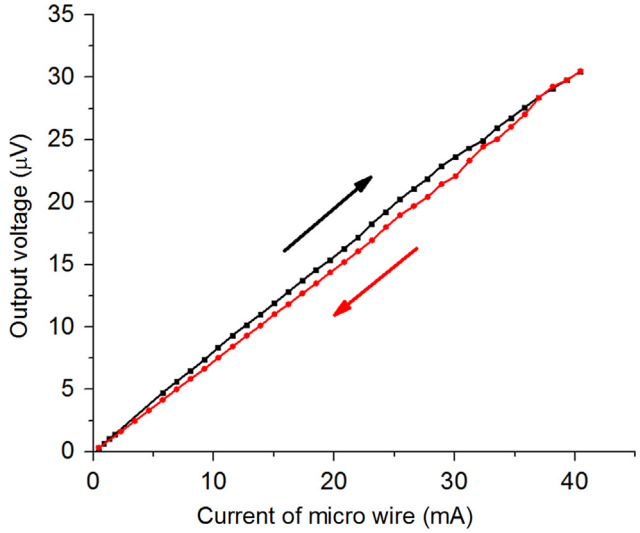

Fig. 3. Output voltage of the magnetic sensor, when applying a current to the microwire. The magnetic field generated by the current in the microwire is perpendicular to the sensor's longitudinal direction.

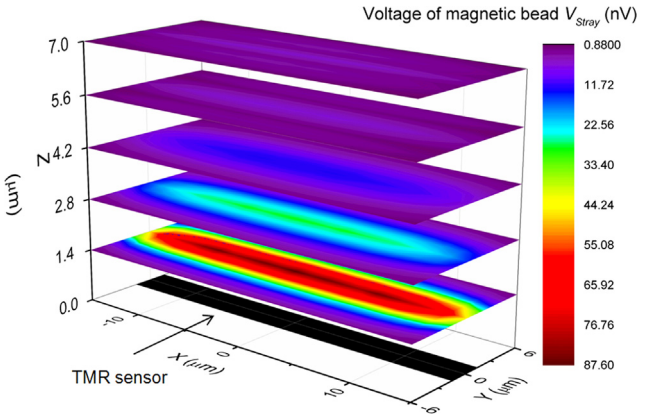

Fig. 4. Simulation results for the voltage, V_{Stray}, of the magnetic sensor caused by the stray field of an individual magnetic bead, when currents of 30 mA and 400 μA are applied to the microwire and sensor, respectively.

When bacteria are attached to the surface of the beads, a part of the sensing space will be occupied by them, yielding a decrease in the sensor signal. In a simple model, this can be taken into account by assuming that a bacterium inside the sensing space reduces the volume of the magnetic beads inside the sensing space by the amount that corresponds to the volume of the bacteria. *E. coli* typically is rod-shaped with a length of 2 μm and a diameter of 1 μm. Depending on the orientation of the bacteria, the signals obtained from a bacterium are 22.74 nV, 20.33 nV and 16.33 nV, when the long axis is aligned along the X direction, the Y direction and the Z direction, respectively.

3.3. Detection of E. coli

Fig. 5a shows the signals of bare magnetic beads and mixtures of magnetic beads with different concentrations of *E. coli*. Once the *E. coli* solution has been added (after 60 s), the signal increases quickly as the beads fill up the sensing space. Eventually, the signal saturates, with the saturation value depending on the *E. coli* concentration. Fig. 5b shows the average saturation values of the signal obtained for three separate measurements of each sample solution. The saturation signal of a bare magnetic bead solution is 1.47 μV, which is in good agreement with the simulation result, since the signal expected from 20 beads inside the sensing space of the TMR sensor is about 1.2 μV. The discrepancy is caused by the magnetic beads located outside the sensing space of the TMR sensor, which were neglected in the calculation of the theoretical value. As shown in Fig. 5b, the average saturation signals of solutions containing *E. coli* with concentrations of 1.29×10^8 bacteria/mL, 3.23×10^8 bacteria/mL and 6.45×10^8 bacteria/mL are 1.09 μV, 0.681 μV and 0.665 μV, respectively.

In order to study the influence of the *E. coli* concentration on the number of *E. coli* attached to beads after the incubation step, the sample solutions were analyzed under a microscope. For each solution, the number of *E. coli* attached to a bead was counted on 15 randomly chosen beads that was studied. The results are shown in Fig. 5b, where each point represents the average value obtained from three different experiments. In the sample with an *E. coli* concentration of 1.29×10^8 bacteria/mL, on average one *E. coli* is attached to one bead. Since the sensing space can hold 20 beads, the number of *E. coli* trapped inside is 20, in this case. The signal obtained from this sample is 1.09 μV, and the difference of 0.38 μV from the signal obtained for bare magnetic beads (1.47 μV) is caused by the 20 bacteria. If we assume that each bacterium inside

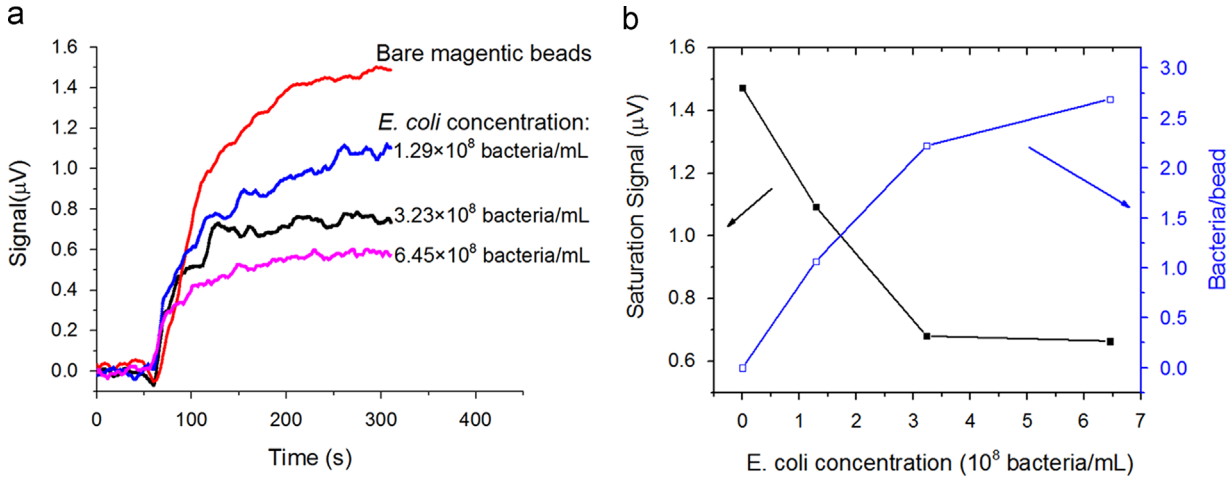

Fig. 5. Detection of *E. coli*: (a) signals of bare magnetic beads and mixtures of magnetic beads with different concentrations of *E. coli*. First, a 1 μL droplet of deionized water is added to stabilize the sensor output voltage. After about 1 min, a 1 μL droplet of sample solution is added. The magnetic beads gradually fill the space on top of the TMR sensor, causing the sensor output to increase gradually. The saturation value of the signal is obtained after about 5 min. Note that the value of the stable sensor output, obtained after adding the droplet of deionized water, has been subtracted from the signal. (b) The average saturation signal versus the *E. coli* concentration (solid square) and the average number of *E. coli* attached a bead versus the *E. coli* concentration (empty square).

the sensing space contributes equally to the signal difference, then the signal of a single *E. coli* is 19 nV. This value is in good agreement with the simulated one, which was found to be between 16.33 nV and 22.74 nV.

The noise voltage, calculated as the standard deviation of the sensor output over a period of 1 min, is 16.2 nV. This is enough to detect a single *E. coli* inside the sensing space, which causes a signal change of 19 nV. As can be seen from Fig. 5(b), when the concentration changes from 0 bacteria/mL to 3.23×10^8 bacteria/mL, the signal decreases almost linearly from 1.47 μV to 0.681 μV. In this range, the sensitivity is 0.244 μV/(10^8 bacteria/mL), resulting in a detection limit of 6.6×10^6 bacteria/mL. The detection range is between 6.6×10^6 bacteria/mL and 3.23×10^8 bacteria/mL. These numbers strongly depend on several parameters. For example, the detection limit depends on the bead-to-bacteria ratio, and the detection range depends on the TMR sensor size, which could be changed by utilizing an array of sensors. In case of small bacteria concentrations, the detection limit can be enhanced by reducing the concentration of the beads. For example, in case of a bead concentration of 3.25×10^2 beads/mL, the detection limit would be 6.6×10^1 bacteria/mL with a range of 3.23×10^3 bacteria/mL. However, such a low concentration requires a method to ensure that there is binding interaction between the beads and bacteria. In order to exploit the potentially high sensitivity of the method, we are currently working on a microfluidic system in which *E. coli* bacteria are concentrated first before adding magnetic beads.

4. Conclusion

We have presented a simple and easy-to-operate magnetoresistive biosensor for the detection of *E. coli*. Compared with magnetic biosensors previously reported, our sensor does not require the sensor's surface to be bio-functionalized. The operating procedure consists of only two steps: First, the bio-analytical sample is mixed with bio-functionalized beads. Second, the solution is applied to the biosensor and the signal is obtained after a few minutes. The total time required for both steps together is about half an hour. While several washing steps are necessary during measurements with sandwich-based magnetic biosensors, washing is not required with our biosensor. Furthermore, there is no need for an external magnetic field source, which is usually employed to magnetize magnetic beads. In our biosensor, the magnetic field is provided by a current through a microwire fabricated on top of the magnetic sensor, which also creates an electromagnetic trap. This greatly reduces the size of the device and simplifies integration. It is also worth noting that our magnetic biosensor can readily be re-used. The biosensor is also easy to clean after a sample is analyzed. Once the current in the microwire is switched off, the beads are no longer trapped and the sensor can be washed. Since no functionalization is needed, it can be used again immediately.

The SNR of the magnetic sensor used in this experiment is high enough to enable the detection of an individual *E. coli* bacterium attached to a bead inside the sensing space. In order to adjust the sensitivity of the biosensor to different biological targets (different sizes), the dimensions and sensitivity of the magnetic sensor can be altered, as well as the size of the magnetic beads.

In summary, this method has several advantages: (i) no functionalization of the chip's surface; (ii) a straightforward, wash-free detection procedure; (iii) re-usability and (iv) simple on-chip integration.

In our future work, we will utilize the new concept in a microfluidic system to improve the detection limit for samples with low bacteria concentrations.

Acknowledgments

The authors wish to thank Dr. Filipe Cardoso of INESC Microsistemas & Nanotechnologias (INESC MN) for his help with the TMR sensor fabrication. The authors also thank Mr. Xiang Yu of KAUST Microwave Lab for his help with the measurement setup.

Appendix A. Supporting information

Supplementary data associated with this article can be found in the online version at: http://dx.doi.org/10.1016/j.bios.2014.03.035.

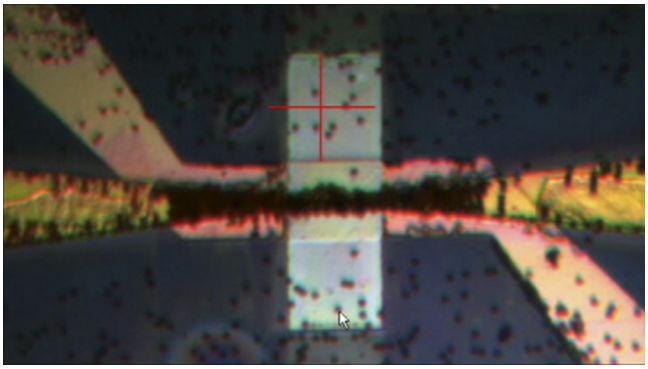

Video S1. A video clip is available online. Supplementary material related to this article can be found online at: http://dx.doi.org/10.1016/j.bios.2014.03.035.

References

Baselt, D.R., Lee, G.U., Natesan, M., Metzger, S.W., Sheehan, P.E., Colton, R.J., 1998. Biosens. Bioelectron. 13, 731–739.

Boyer, T.H., 1988. Am. J. Phys. 56, 688.

Buchatip, S., Ananthanawat, C., Sithigorngul, P., Sangvanich, P., Rengpipat, S., Hoven, V.P., 2010. Sensors Actuators B: Chem. 145 (1), 259–264.

Chan, K.Y., Ye, W.W., Zhang, Y., Xiao, L.D., Leung, P.H.M., Li, Y., Yang, M., 2013. Biosens. Bioelectron. 41, 532–537.

de Boer, B.M., Kahlman, J.A.H.M., Jansen, T.P.G.H., Duric, H., Veen, J., 2007. Biosens. Bioelectron. 22 (9–10), 2366–2370.

Gaster, R.S., Hall, D.A., Wang, S.X., 2011a. Nano Lett. 11 (7), 2579–2583.

Gaster, R.S., Hall, D.A., Wang, S.X., 2011b. Lab Chip 11 (5), 950.

Gaster, R.S., Xu, L., Han, S.-J., Wilson, R.J., Hall, D.A., Osterfeld, S.J., Yu, H., Wang, S.X., 2011c. Nat. Nanotechnol. 6 (5), 314–320.

Gooneratne, C.P., Giouroudi, I., Kosel, J., 2012. Sensor Letters 10 (3–4), 3–4.

Gooneratne, C.P., Yassine, O., Giouroudi, I., Kosel, J., 2013. IEEE Trans. Magn. 49 (7), 3418–3421.

Guo, X., Lin, C.-S., Chen, S.-H., Ye, R., Wu, V.C.H., 2012. Biosens. Bioelectron. 38 (1), 177–183.

Lang, X.-Y., Fu, H.-Y., Hou, C., Han, G.-F., Yang, P., Liu, Y.-B., Jiang, Q., 2013. Nat. Commun. 4, 2169.

Lazcka, O., Campo, F.J.D., Muñoz, F.X., 2007. Biosens. Bioelectron. 22 (7), 1205–1217.

Li, F., Kosel, J., 2013. IEEE Trans. Magn. 49 (7), 3492–3495.

Mechery, S.J., Zhao, X.J., Wang, L., Hilliard, L.R., Munteanu, A., Tan, W., 2006. Chem. – Asian J. 1 (3), 384–390.

Narsaiah, K., Jha, S.N., Bhardwaj, R., Sharma, R., Kumar, R., 2011. J. Food Sci. Technol. 49 (4), 383–406.

Shen, W., Liu, X., Mazumdar, D., Xiao, G., 2005. Appl. Phys. Lett. 86 (25), 253901.

Su, X.-L., Li, Y., 2004. Biosens. Bioelectron. 19 (6), 563–574.

Velusamy, V., Arshak, K., Korostynska, O., Oliwa, K., Adley, C., 2010. Biotechnol. Adv. 28 (2), 232–254.